Published in final edited form as:

Nat Mater. 2015 March ; 14(3): 352–360. doi:10.1038/nmat4157.

Light-triggered *in vivo* Activation of Adhesive Peptides Regulates Cell Adhesion, Inflammation and Vascularization of Biomaterials

Ted T. Lee[1,2], **José R. García**[1,2], **Julieta Paez**[3], **Ankur Singh**[1,2,4], **Edward A. Phelps**[1,2], **Simone Weis**[3], **Zahid Shafiq**[3], **Asha Shekaran**[1,2], **Aránzazu del Campo**[3], and **Andrés J. García**[1,2,*]

[1]Woodruff School of Mechanical Engineering, Georgia Institute of Technology, Atlanta, Georgia 30332, USA

[2]Petit Institute for Bioengineering and Bioscience, Georgia Institute of Technology, Atlanta, Georgia 30332, USA

[3]Max-Planck-Institut für Polymerforschung, Mainz 55128, Germany

[4]Sibley School of Mechanical and Aerospace Engineering, Cornell University, Ithaca, New York 14853, USA

Abstract

Materials engineered to elicit targeted cellular responses in regenerative medicine must display bioligands with precise spatial and temporal control. Although materials with temporally regulated presentation of bioadhesive ligands using external triggers, such as light and electric fields, have been recently realized for cells in culture, the impact of *in vivo* temporal ligand presentation on cell-material responses is unknown. Here, we present a general strategy to temporally and spatially control the *in vivo* presentation of bioligands using cell adhesive peptides with a protecting group that can be easily removed via transdermal light exposure to render the peptide fully active. We demonstrate that non-invasive, transdermal time-regulated activation of cell-adhesive RGD peptide on implanted biomaterials regulates *in vivo* cell adhesion, inflammation, fibrous encapsulation, and vascularization of the material. This work shows that triggered *in vivo* presentation of bioligands can be harnessed to direct tissue reparative responses associated with implanted biomaterials.

*Correspondence and requests for materials should be addressed to A.J.G. andres.garcia@me.gatech.edu.

AUTHOR CONTRIBUTION

TTL and JRC conducted all experiments, collected data and performed data analysis. JP, SW, and ZS synthesized and characterized caged compounds. ASingh performed *in vivo* uncaging efficiency study, and AShekaran and EAP assisted with hydrogel development and implantation procedures. AJG and AdC developed the concept, and together with TTL contributed to the planning and design of the project. TTL, AdC, and AJG wrote the manuscript and all authors discussed the results and commented on the manuscript.

COMPETING FINANCIAL INTERESTS

The authors declare no competing financial interests.

Cell adhesion to the extracellular matrix (ECM) provides mechanical support and biochemical signals regulating diverse cell behaviors critical to tissue morphogenesis, homeostasis and repair [1,2]. Far from static, the adhesion process comprises dynamic interactions over multiple time and length scales, spanning nano-scale integrin receptor-ECM ligand binding (seconds), clustering of integrins with cytoskeletal elements into sub-micron/micron-scale focal adhesions (minutes-hours), activation of signaling pathways and transcriptional programs (hours-days), and meso/macro-scale ECM remodeling and tissue organization (days-weeks) [3,4]. Cell-ECM adhesion is tightly regulated, and misregulated interactions often result in pathological conditions such as developmental defects, wound healing deficiencies and tumorigenesis [2,5]. In an analogous fashion, the engineering of materials to elicit desired cellular responses in regenerative medicine will require precise control over spatiotemporal bioligand presentation [6–10]. Despite progress in the fabrication of biomaterials with exquisite spatial control of bioligand display [11–13], materials with temporally regulated presentation of bioadhesive ligands using external triggers (e.g., temperature, light, electric field) under *in vitro* culture conditions have only been recently realized [14–21]. A standing question in the biomaterials field is whether temporal presentation of bioligands on implanted materials can be exploited to modulate *in vivo* cell behaviors to elicit targeted reparative responses. Because biological responses to implanted materials comprise temporal cascades, control over *in vivo* material properties such as presentation of bioactive ligands represents a powerful and novel approach to engineer host responses to implanted materials. In the work presented here, we establish a general strategy to temporally and spatially control the *in vivo* presentation of bioligands using a synthetic cell-adhesive RGD (Arg-Gly-Asp) peptide with a protecting group (‘cage’) on its integrin receptor-binding site that can be easily removed with light at prescribed wavelengths to render the RGD peptide fully active. Furthermore, we demonstrate that non-invasive, transdermal activation of the cell-adhesive RGD peptide on biomaterials at particular time points after implantation regulates *in vivo* cell adhesion, inflammation, and vascularization of the material.

Light-triggered activation of caged RGD peptide

We engineered light-triggerable cell adhesive materials using the cyclic RGD peptide cyclo(Asp-D-Phe-Lys-Arg-Gly) modified with a 3-(4,5-dimethoxy-2-nitrophenyl)-2-butyl ester (DMNPB) photolabile caging group on the carboxylic side group of the Asp residue [14]. Upon exposure to light (λ ~ 350–365 nm), the caging group is released resulting in the presentation of the active cyclic RGD peptide (Fig. 1a). We first examined presentation of cell adhesive peptides on the surface of poly(ethylene glycol) di-acrylate (PEGDA) hydrogels, a widely used biomaterial with excellent non-fouling and cell adhesion-resistant properties. For tethering onto hydrogels, adhesive peptides were first acrylated using a commercial reagent. MALDI mass spectrometry demonstrated acrylation of the caged RGD peptide as demonstrated by the predicted shift in mass/charge ratio (Fig. S1). Hydrogels presenting adhesive peptides were generated by covalently incorporating acrylated peptides (2% w/v) onto the surface of bulk PEGDA hydrogels via free-radical polymerization.

To test the ability to trigger cell adhesion to these materials *in vitro*, peptide-modified and unfunctionalized PEGDA hydrogels were either exposed to UV light (λ = 351 nm, 20

mW/cm^2) for 10 minutes or not exposed. Fibroblasts were then cultured on these hydrogels for 24 hours, and adherent cell numbers and spreading were evaluated by image analysis. Very few cells adhered to unmodified PEGDA, confirming the cell adhesion-resistant background provided by this material (Fig. 1b). Hydrogels presenting caged RGD peptide that were not exposed to light also supported very low numbers of adherent cells, and the few cells that adhered were round, similar to the levels of cell adhesion to unmodified PEGDA (Fig. 1b). In contrast, hydrogels presenting caged RGD peptide that were UV-exposed to remove the caging group supported high numbers of well spread, adherent cells, similar to those on hydrogels presenting control cyclic RGD peptide (Fig. 1b). As expected, no differences in cell adhesion were observed between UV-exposed and non-exposed gels that presented control RGD peptide or unmodified PEGDA. Quantification of the number of adherent cells over multiple fields demonstrated equivalent low levels of cell adhesion between non-UV exposed caged RGD peptide-presenting gels and unmodified PEGDA ($p = 0.5$, Fig. 1c). UV-exposed gels presenting caged RGD peptide supported 4-fold higher adherent cell densities ($p < 0.01$). No differences in cell density ($p = 0.08$) or spreading (892 ± 83 μm^2 vs. 871 ± 91 μm^2 [mean ± stdev], p=0.73) were observed between UV-exposed caged RGD-presenting gels and hydrogels presenting control RGD peptide, demonstrating that the uncaged RGD peptide displays full adhesive activity. Finally, low levels of adhesion were observed on hydrogels presenting a scrambled RGD peptide (RDG), showing that cell adhesion in this system is specific to the presence of the RGD sequence.

Transdermal activation of caged bioligands

We selected light as the trigger for the display of bioactive molecules because this stimulus offers unparalleled spatiotemporal control and the potential to use transdermal light exposure to remove the caging group *in vivo* in a non-invasive fashion. For *in vivo* studies in mice, we used UV-A light ($\lambda = 351$ nm, 20 mW/cm^2) for short exposures (10 minutes) to minimize photo-damage. This longer wavelength produces less damage than UV-B and UV-C and has been used for transdermal photopolymerization [22]. Preliminary experiments demonstrated no skin photo-damage or adverse effects at the doses used.

We measured UV attenuation through murine skin in our experimental set-up using a photometer. UV attenuation increased with the thickness of the skin sample and follows an exponential decay as predicted by Beer's Law (Fig. S2). For the skin from the murine dorsum where the biomaterial samples were implanted, we estimate 90% attenuation of the UV light.

We next analyzed the stability and uncaging efficiency of the caged RGD peptide-functionalized gels following subcutaneous implantation in mice and transdermal UV exposure. For these studies, we used an acrylate derivative of bis-(5-carboxymethoxy-2-nitrobenzyl)ether (CMNB)-caged fluorescein as an analogue for the caged RGD peptide (Fig. S3). This caged fluorescein has low fluorescence when the caging group is present but displays high fluorescence when the caging group is removed. PEGDA gels presenting UV-exposed or non-exposed caged fluorescein and unfunctionalized gels were implanted into mice, and at prescribed times the area of the skin corresponding to where the implant was located was either exposed to UV light or left untreated (Fig. S4). After sacrifice at 7 or 14

days, the implants were recovered and the fluorescence intensity, corresponding to the extent of uncaging, was quantified. Hydrogels presenting caged fluorescein that were not exposed to UV light exhibited minimal fluorescence after 7 and 14 days implantation (Fig. S4), equivalent to background fluorescence levels associated with unmodified PEGDA gels. Hydrogels that were UV-exposed transdermally immediately after implantation exhibited 10-fold higher fluorescence levels compared to implants presenting caged fluorescein that were not UV exposed ($p < 0.0001$, Fig. S4), demonstrating that transdermal UV exposure removes the caging group to trigger *in vivo* presentation of the caged molecule. Importantly, there are no differences in the fluorescence signal among hydrogels presenting caged fluorescein exposed to UV prior to implantation (pre-exposed) and hydrogels presenting caged fluorescein exposed to UV transdermally immediately after implantation (Day 0) or at 14 days post-implantation (Day 14) (Fig. S4). These results demonstrate that both caged and uncaged compounds remain stable *in vivo* and that transdermal uncaging efficiency is high and independent of implantation time.

Transdermal activation of cell adhesion

Having established the ability to trigger transdermal uncaging of the bioligand, we assessed whether transdermal activation of caged RGD peptide-tethered hydrogels regulates *in vivo* cell adhesion (Fig. 2). Unmodified PEGDA gels and hydrogels presenting control or caged RGD were implanted subcutaneously in mice. Immediately after wound closure, implants were either exposed to UV transdermally or not exposed. Twenty-four hours after implantation, hydrogels were carefully explanted and adherent cells were stained for DNA, neutrophil (NIMP-R14) and macrophage (CD68) markers using fluorescent antibodies and analyzed by microscopy (Fig. 2b, c). Few cells adhered to unexposed or UV-exposed unfunctionalized PEGDA hydrogels, showing that UV exposure does not alter cell adhesion to these non-fouling materials. Equivalent low cell numbers were observed on hydrogels presenting caged RGD peptide which were not UV-exposed, showing that the caged RGD peptide retains low cell adhesive activity *in vivo*. In contrast, hydrogels presenting caged RGD peptide which were transdermally exposed to UV light exhibited high numbers of adherent cells that were uniformly distributed over the biomaterial surface ($p < 0.001$), equivalent to cell numbers and distribution on control RGD or caged RGD peptide that was UV exposed prior to implantation. Immunostaining of adherent cells showed that the majority of the recruited cells were neutrophils (NIMP-R14+) with macrophages (CD68+) comprising the rest of the adherent cells, consistent with the expected inflammatory cell profile at this acute time point [23]. Taken together, these results demonstrate transdermal activation of caged RGD peptide to trigger *in vivo* acute cell adhesion to biomaterials.

We also examined transdermal activation of cell adhesion to a different class of PEG hydrogel. PEG-maleimide hydrogels offer significant advantages over PEGDA hydrogels such as well-defined hydrogel structure, stoichiometric incorporation of adhesive peptides, and flexibility in using protease-degradable cross-links that allow for robust cell spreading and migration within the gel [24]. For this follow-up study, we synthesized a cysteine-containing caged RGD peptide for reacting with maleimides in 4-arm PEG-maleimide macromers (Fig. S5a, b). Importantly, we also generated a caged RDG scrambled peptide to serve as a stringent non-adhesive control peptide for the caged RGD peptide. Peptide-

functionalized hydrogels were implanted subcutaneously and exposed to UV light transdermally immediately after wound closure. Twenty-four hours later, the hydrogels were explanted and the number of cells adherent to the material was quantified by image analysis. Consistent with our observations for the PEGDA gels, PEG-maleimide gels presenting caged RGD peptide that were not UV-exposed had background levels of adherent cells, equivalent to hydrogels presenting control RDG peptides (Fig. S5c). Hydrogels that had been exposed to transdermal UV light had approximately 3-fold higher cell numbers than non-UV exposed controls (Fig. S5c, $p < 0.0001$). No differences in cell numbers were detected among hydrogels presenting caged RGD peptide that were exposed to UV transdermally or exposed to UV light prior to implantation and hydrogels presenting control cyclic RGD peptide. Importantly, hydrogels presenting the caged scrambled RDG peptide exhibited low numbers of adherent cells regardless of whether they received UV light exposure or not. These results demonstrate control of *in vivo* cell adhesion to biomaterials via UV light-based activation of RGD peptides.

In vivo spatial patterning of adhesive ligands

A major advantage of the use of light as an external trigger is the ability to spatially pattern light exposure to control the spatial activation of caged bioligands. To demonstrate this application, we implanted PEG hydrogels presenting either caged RGD or caged RDG peptides subcutaneously and exposed them to UV light transdermally through a mask containing a 0.9 mm hole centered over the area where the hydrogel was implanted (Fig. 3a). The next day, hydrogels were explanted and stained for cell nuclei (DNA). For hydrogels presenting caged RGD peptides, high cell numbers were observed directly at the site of UV light exposure and cell numbers decreased to background levels away from the irradiation spot (Fig. 3b). For hydrogels presenting caged RDG peptide, adherent cell numbers were low and independent of position. Fig. 3c presents a composite image of photographs of adherent cells at different positions along the hydrogel surface showing high numbers of adherent cells localized to the exposure spot (yellow circle) and low levels of adherent cells outside the exposure point. Quantification of cell numbers at different spatial positions on the hydrogel shows monotonic decreases in cell density with distance away from the irradiation spot (Fig. 3c). These results demonstrate spatial control over *in vivo* RGD presentation and cell patterning via transdermal illumination.

Activation of RGD peptide modulates fibrous encapsulation

We next examined whether time-regulated presentation of RGD peptide modulates chronic inflammatory responses to biomaterials. We used PEGDA hydrogels because these gels are non-degradable and elicit a uniform collagenous fibrous capsule allowing direct comparisons among different exposure conditions. Unmodified PEGDA hydrogels and gels presenting control RGD or caged RGD peptide were implanted subcutaneously in mice. At 0, 7 or 14 days post-implantation, implants were exposed to UV transdermally. After sacrifice at day 28, implants and associated tissues were carefully explanted, embedded in plastic, and processed for Masson's trichrome staining. Fig. 4a presents sections of the biomaterial-tissue interface showing the collagenous fibrous capsule characteristic of chronic inflammation to biomaterials [23,25]. The fibrous capsule thickness (yellow bar) was

quantified as a measure of chronic inflammation (Fig. 4b). Unmodified PEGDA gels elicited thin capsules, whereas hydrogels presenting control RGD peptide produced fibrous capsules that were 60% thicker than capsules for unmodified PEGDA ($p < 0.001$). This result shows that static presentation of RGD adhesive peptides on biomaterials promotes chronic inflammation and fibrous encapsulation. Additionally, no differences in fibrous capsule thickness were observed between UV-exposed and non-UV exposed subjects for these control implant groups (Fig. S6), demonstrating that transdermal UV exposure does not alter chronic inflammatory responses to these materials. Hydrogels presenting caged RGD peptide which were not exposed to UV light had thin fibrous capsules, equivalent to those for unmodified gels (Fig. 4a, b). In contrast, hydrogels presenting caged RGD peptide which were irradiated immediately after implantation (day 0) exhibited fibrous capsules that were 50% thicker than capsules for gels with caged RGD peptide which were not exposed to UV light ($p < 0.01$). The fibrous capsule thickness for caged RGD peptide-tethered gels exposed at day 0 was equivalent to the capsule thickness for gels with control static RGD peptide ($p = 0.12$). Hydrogels presenting caged RGD peptide transdermally exposed to UV at either 7 or 14 days post-implantation exhibited fibrous capsules that were 50% thinner than those for hydrogels presenting caged RGD peptide that were irradiated immediately after implantation ($p < 0.05$), and the capsule thickness was not different from that for unmodified hydrogels or gels presenting caged RGD peptides which were not exposed to UV light ($p = 0.2$). These results demonstrate that delayed presentation of adhesive ligands on implanted biomaterials significantly reduces chronic inflammation and fibrosis.

In vivo RGD activation triggers vascularization of hydrogels

Having demonstrated that time-dependent *in vivo* activation of RGD peptide presentation modulates cell adhesion and inflammation at the tissue-biomaterial interface, we next examined whether light-based activation of adhesive peptides could trigger 3-D cell invasion and vascularization of implanted biomaterials. We used PEG-maleimide hydrogels with precise incorporation of adhesive peptides and protease-degradable cross-links that allow for robust cell spreading and migration within the gel [24]. We first examined *in vitro* cell invasion into these biomaterials by polymerizing peptide-functionalized hydrogels around a cell pellet and evaluating cell sprouting into the gel (Fig. S7). Fibroblast sprouting into the gel was completely dependent on the presentation of adhesive RGD peptide as shown by significant cell invasion into the gel for control RGD peptide and no cell outgrowth for scrambled RDG control peptide ($p < 0.0001$). UV exposure of hydrogels presenting caged RGD peptide resulted in significant fibroblast sprouting ($p < 0.05$), whereas no cell outgrowth was observed in gels that were not exposed to UV light, demonstrating light-triggered cell invasion into these biomaterials.

We have shown that PEG-maleimide hydrogels with adhesive peptides and protease-degradable cross-links are suitable vehicles for controlled delivery of VEGF that direct *in vivo* vascularization [27]. In this system, VEGF is released upon protease-dependent degradation of the hydrogel. To demonstrate that VEGF is retained within the hydrogel over time, we performed an *ex vivo* VEGF release experiment. Fluorescently-labeled VEGF was incorporated within PEG hydrogels and incubated in either buffer or buffer containing collagenase to degrade the hydrogel. At defined time points, VEGF released into the

surrounding media was measured to quantify VEGF release. More than 60% of the incorporated VEGF remains within the hydrogel over 7 days in culture (Fig. S8). However, in the presence of collagenase, the gel degrades releasing the incorporated VEGF. These results demonstrate that VEGF is retained with the hydrogel network and released in response to collagenase-mediated degradation.

To examine triggerable control over *in vivo* vascularization, PEG-maleimide hydrogels presenting caged RGD or RDG peptides, protease-degradable crosslinks, and VEGF vasculogenic protein were polymerized directly into subcutaneous pockets in mice. At 0 or 7 days post-implantation, implants were exposed to UV light transdermally. Following sacrifice at day 14, hydrogels were explanted, stained for different cell markers, and analyzed by confocal microscopy to examine cell infiltration and vascularization within the hydrogel. As shown by cell nuclei staining, all implanted hydrogels exhibited high cell numbers within the implant with no gross differences for cell infiltration among hydrogel type (RGD, RDG) or UV exposure condition (Fig. 5a). This observation is in agreement with previous reports [26–28]. Staining for inflammatory cell markers revealed that the large majority of cells were macrophages and no staining for neutrophils was evident, which is the expected inflammatory cell profile at this time point [23,25]. Importantly, hydrogels presenting caged RGD peptide that had been UV-exposed transdermally at day 0 or day 7 contained many tubular structures that stained positive for the endothelial cell marker CD31 and smooth muscle cell marker αSMA (Fig. 5a and S9), indicating vascularization of these hydrogels. In contrast, hydrogels presenting caged RGD peptide which had not been exposed to UV light exhibited diffuse staining for CD31 and αSMA, and no tubular structures resembling blood vessels were observed (Fig. 5a and S9). Likewise, hydrogels presenting caged scrambled RDG peptide showed diffuse CD31 and αSMA staining and no evidence of blood vessels for any UV exposure condition. These results demonstrate that UV-light triggered activation of RGD peptides promotes vascularization of these hydrogels.

To examine whether hydrogels presenting caged RGD peptide supported formation of functional blood vessels, VEGF-containing hydrogels were polymerized *in situ* subcutaneously and exposed to UV light transdermally at day 0 or 7 post-implantation. At day 14, DyLight488-conjugated tomato lectin was infused intravenously to label functional vasculature, and implants were recovered and imaged by confocal microscopy as whole mount preparations. Image projections from 3-D reconstructions and vessel counts clearly show functional vessels within hydrogels presenting control RGD peptide and sparse vessels for gels presenting scrambled RDG peptide (Fig. 5b, c). This result shows that adhesive RGD peptide is required for the *in vivo* formation of functional blood vessels within implanted hydrogels, consistent with our previous reports [26,27]. Gels presenting caged RGD peptides which were not exposed to UV had few blood vessels, with equivalent low vessel counts as gels presenting scrambled peptides. In contrast, hydrogels presenting caged RGD peptides which were UV exposed transdermally exhibited robust functional blood vessel formation and had 3 times more vessels than non-UV exposed gels ($p < 0.05$). There are no significant differences in blood vessel density between hydrogels presenting caged RGD peptides which were exposed to UV light at day 0 or day 7 ($p = 0.1$) or between these groups and the control RGD peptide ($p = 0.06$). Taken together, the immunostaining and lectin

perfusion results demonstrate that *in vivo* triggering of cell adhesive RGD peptides regulates vascularization of VEGF-containing hydrogels.

The present study establishes a general strategy to spatially and temporally control the *in vivo* presentation of bioligands using bioactive peptides with a protecting group that can be easily removed via transdermal light exposure to render the peptide fully active. This strategy is fundamentally different from other work using light for *in vivo* drug delivery and self-assembly applications that relies on energy-driven physical changes in the material [29–31]. We demonstrate that non-invasive, transdermal activation of the cell adhesive RGD peptide on implanted biomaterials regulates *in vivo* cell adhesion and spatial patterning, inflammation, fibrous encapsulation, and vascularization of the material. This work shows that triggered *in vivo* presentation of bioligands can be harnessed to direct tissue reparative responses associated with implanted biomaterials. As shown in this study, light-regulated ligand activation can be exploited to promote desired healing responses (e.g., cell adhesion, vascularization) while avoiding deleterious biological consequences (e.g., inflammation, fibrous encapsulation). We targeted the cell adhesive RGD peptide because of its critical importance in binding to several integrin receptors associated with host responses to biomaterials. Delayed activation of RGD presentation reduced the thickness of the fibrous capsule around the implanted biomaterial. A possible explanation for this reduced chronic inflammatory response is altered adhesion and signaling by neutrophils and macrophages recruited to the biomaterial surface. Blocking of RGD peptide binding to $\alpha_M\beta_2$ (Mac-1) integrin among others on macrophages results in reduced pro-inflammatory cytokine secretion in cultured cells and thinner fibrous capsules around polymeric implants [32]. The RGD peptide also binds the $\alpha_V\beta_3$ integrin, which plays a central role in endothelial cell function and vascularization [33].

The present research focused on a UV-labile cage. This light trigger is limited for *in vivo* applications in terms of spatial resolution and depth of penetration because of the significant attenuation and scattering due to the optical properties of biological tissue and target biomaterials. However, we expect that photosensitive groups with near-infrared response regimes would provide for enhanced tissue penetration and reduced scattering. Because of the high degree of spatiotemporal control afforded by light and the availability of various photosensitive groups, we anticipate that this strategy will find widespread adoption in biomedical applications requiring precise spatiotemporal bioligand presentation. Exemplary applications include directed host-material integration and vascularization, antigen recognition and tolerance induction for immunoengineering, targeting of nano/microparticles to local sites in cancer and inflammatory disorders, and generation of stem cell niches with dynamic bioligand presentation.

METHODS

RGD peptides and hydrogels

Synthetic protocols are included in SI. Synthesis of the caged RGD peptide has been described [14]. Caged RDG peptide and fluorescein and cysteine-containing peptides were synthesized using similar methods described in SI. Acrylated caged RGD peptide was generated by reacting 1.1:1 molar ratio acryl-PEG-SVA (Laysan Bio) with the primary

amine of the caged RGD peptide for 4 hours in $NaHCO_3$ buffer (pH = 8.2). PEGylated control RGD and scrambled RDG peptides (Peptides International) were generated in the same fashion. Acrylated peptides were dialyzed and lyophilized for storage at −20°C. Peptide acrylation was confirmed by MALDI-mass spectrometry.

PEGDA hydrogels were prepared using a mixture of 10% PEGDA (3400 Da, Laysan Bio) and 0.05% Irgacure 2959 (BASF) in phosphate-buffered saline. These precursors were cross-linked in a sterilized silicon mold mounted to a glass coverslip sealed by a Sigmacote-coated microscope slide. Hydrogels were cross-linked using a UV light table (λ = 351 nm, 10 mW/cm^2) for 15 minutes. Bulk gels were functionalized with a thin top gel (25 μL) consisting of 8% PEGDA and 2% acrylated peptide and cross-linked via free radical polymerization using TEMED and ammonium persulfate. This chemical polymerization resulted in a 50 μm thick functionalized gel that was mechanically integrated onto the bulk hydrogel.

For PEG-maleimide gels, 4-arm PEG-maleimide macromers (20 kDa, Laysan Bio) were functionalized with cysteine-containing RGD or RDG peptides and cross-linked with a protease-degradable peptide (GCRDVPMSMRGGDRCG) as previously described [24]. The final peptide density in these gels was 2.0 mM.

Hydrogels were prepared as disks (8 mm diameter, 2 mm thick) or polymerized directly *in situ* (75 μL). Hydrogels were prepared using sterile filtered components under sterile conditions. Precursor solutions and hydrogels were tested using LAL assay and found to be endotoxin-free, with values well below the 20 EU/per device as specified by ISO10993 standards.

UV exposure system

A custom-built UV exposure system consisting of an X-Cite 120 Arc Lamp (Exfo), collimator, band-pass filter, VS14/25 shutter and VMM-T1 Shutter Driver Controller (Uniblitz) was used for all *in vitro* and *in vivo* experiments.

In vitro cell adhesion and outgrowth

NIH3T3 fibroblasts (20,000/cm^2) were cultured overnight on peptide-functionalized or unmodified PEGDA hydrogels. Cells were labeled with the Live/Dead assay (Invitrogen) and fluorescence images were acquired in a Nikon TE-300 microscope with a 20X objective and Spot RT digital camera. Cell densities were quantified using in-house macros in ImageJ.

IMR-90 fibroblasts were detached, pelleted, and pipetted into polymerizing PEG-maleimide gels to encapsulate the cell pellet within gel. After 30 minutes, cell media was added. Cell outgrowth sprout length was analyzed at 24 hours post-encapsulation using ImageJ.

Implantation of hydrogels and transdermal UV exposure

Sterile, endotoxin-free hydrogels (8 mm diameter, 1 mm thick), were implanted subcutaneously (2 implants/mouse) following IACUC-approved procedures in 6–10 week old male Balb/c mice (Jackson Laboratories). The custom-built UV exposure system was used for transdermal irradiation. At prescribed time points, mice were anesthetized and the

skin in the vicinity of the implant was treated with depilatory cream to remove hair and exposed to UV light (λ = 351 nm, 20 mW/cm^2) for 10 minutes.

To measure UV attenuation through skin, the dermal layer of the ventral and dorsal sides of Balb/c mice euthanized following IACUC-approved methods was removed and cut into 2 cm × 2 cm squares and kept in ice cold PBS. Dermal layer thickness was then measured in triplicate utilizing a digital caliper (Storm Equipment). Percent UV attenuation was measured in triplicate for each piece of derma using a UVX radiometer (UVP). For Beer's law analysis, data for UV attenuation as a function of skin thickness was fit with a single exponential curve using GraphPad Prism 6.0.

For *in vivo* uncaging efficiency studies, CMNB-caged fluorescein was acrylated with acryl-PEG-SVA using 1:1.1 ratio and DMF/DIPEA coupling conditions (SI). Caged fluorescein-functionalized PEGDA hydrogels were generated in the same manner as described for RGD peptide-presenting hydrogels. Pre-exposed and unexposed caged fluorescein-presenting gels and control bare hydrogels were implanted subcutaneously in mice, and exposed to UV transdermally at defined time points. Following sacrifice, implants were recovered and fluorescence imaged using a Nikon TE-300 microscope and quantified using ImageJ.

For transdermal patterning studies, an exposure mask consisting of a large sheet of aluminum foil with a central 0.9 mm hole created with a 20-gauge needle was prepared. Anesthetized mice were exposed to UV light for 10 minutes through the mask gently pressed onto the skin with the hole aligned over the center of the implanted hydrogel. At day 1, mice were euthanized and implants were extracted and washed in cold PBS followed by fixation in 4% paraformaldehyde for 30 minutes. Cells were stained with DAPI and explants were imaged using a Nikon Eclipse Ti microscope connected to a Nikon C2+ confocal module. Cell adhesion and patterning were quantified using ImageJ.

For histological analyses of fibrous encapsulation, explants were fixed in formalin and embedded using the Immunobed Kit (Polysciences). Tissue sections (2 μm thick) were stained Mason's trichrome stain, imaged, and collagenous capsule thickness was analyzed in ImageJ.

Vascularization

RGD or RDG peptide-functionalized PEG-maleimide macromers were mixed with Recombinant human VEGF-165 (R&D, 10 μg/mL final concentration) and cross-linking peptides, and the resulting mixture (75 μL) was directly polymerized within subcutaneous pockets in the backs of mice. At day 14, mice were euthanized and the hydrogels explanted, washed with ice cold PBS, fixed in 10% formalin overnight. Whole-mounted implants were cut in half, blocked with 3% bovine serum albumin, and stained for either CD31 and α-smooth muscle actin or CD68 and NIMP-R14 (Abcam). The secondary antibodies used were either conjugated to AlexaFluor488 or AlexaFluor555 (Invitrogen). Explants were then stained with DAPI and imaged using a Nikon Eclipse Ti microscope connected to a Nikon C2+ confocal module. 2-D images over the sample thickness were acquired to generate 3-D reconstructions using a Nikon C2+ laser scanning confocal head on a Nikon Eclipse-Ti microscope and Elements software in order to cells and structures within the hydrogel.

To label functional blood vessels, DyLight488-conjugated tomato lectin (1 mg/mL) was injected through the tail vein and allowed to circulate for 20 minutes. Mice were then perfused with 0.4% papaverine in saline through the left ventricle and bled through the inferior vena cava. The circulatory system was then perfused with 50 mL of 1% papaverine-containing saline for 5 minutes. Hydrogels were explanted, fixed in formalin, and whole mounted on microscope slides. 2-D images over the sample thickness were acquired to generate 3-D reconstructions using a Nikon C2+ laser scanning confocal head on a Nikon Eclipse-Ti microscope and Elements software in order to image vessels within the hydrogel.

Statistical analyses

Statistical analyses were performed using GraphPad Prism 6.0. For normally distributed data with equal variances, one-way ANOVA with Tukey's multiple comparison test was used. For data that did not satisfy the requirements for ANOVA, non-parametric Kruskal-Wallis tests with Bonferroni-Dunn's multiple comparison tests were used. A p-value < 0.05 was considered significant. Non-linear regression analyses were also performed in GraphPad Prism 6.0.

Supplementary Material

Refer to Web version on PubMed Central for supplementary material.

Acknowledgments

This work was supported by the Materials World Network Program grants DFG AOBJ 569628 (AdC) and NSF DMR-0909002 (AJG) and the National Institutes of Health (NIH) grants R01-AR062368 and R01-AR062920 (AJG). TTL and JRG were supported by the Cell and Tissue Engineering NIH Biotechnology Training Grant (T32 GM-008433).

References

1. Hynes RO. The extracellular matrix: not just pretty fibrils. Science. 2009; 326(5957):1216–1219. [PubMed: 19965464]
2. Hynes RO. Integrins: bidirectional, allosteric signaling machines. Cell. 2002; 110(6):673–687. [PubMed: 12297042]
3. Wolfenson H, Lavelin I, Geiger B. Dynamic regulation of the structure and functions of integrin adhesions. Dev Cell. 2013; 24(5):447–458. [PubMed: 23484852]
4. Schiller HB, Fassler R. Mechanosensitivity and compositional dynamics of cell-matrix adhesions. EMBO Rep. 2013; 14(6):509–19. [PubMed: 23681438]
5. Kumar S, Weaver VM. Mechanics, malignancy, and metastasis: the force journey of a tumor cell. Cancer Metastasis Rev. 2009; 28(1–2):113–127. [PubMed: 19153673]
6. Ranga A, Lutolf MP. High-throughput approaches for the analysis of extrinsic regulators of stem cell fate. Curr Opin Cell Biol. 2012; 24(2):236–244. [PubMed: 22301436]
7. Fisher OZ, Khademhosseini A, Langer R, Peppas NA. Bioinspired materials for controlling stem cell fate. Acc Chem Res. 2010; 43(3):419–428. [PubMed: 20043634]
8. Pashuck ET, Stevens MM. Designing regenerative biomaterial therapies for the clinic. Sci Transl Med. 2012; 4(160):160sr164.
9. Rice JJ, Martino MM, De Laporte L, Tortelli F, Briquez PS, Hubbell JA. Engineering the regenerative microenvironment with biomaterials. Adv Healthc Mater. 2013; 2(1):57–71. [PubMed: 23184739]

10. Vogel V, Sheetz M. Local force and geometry sensing regulate cell functions. Nat Rev Mol Cell Biol. 2006; 7(4):265–275. [PubMed: 16607289]
11. DeForest CA, Polizzotti BD, Anseth KS. Sequential click reactions for synthesizing and patterning three-dimensional cell microenvironments. Nat Mater. 2009; 8(8):659–664. [PubMed: 19543279]
12. Lohmuller T, Aydin D, Schwieder M, Morhard C, Louban I, Pacholski C, et al. Nanopatterning by block copolymer micelle nanolithography and bioinspired applications. Biointerphases. 2011; 6(1):MR1–12. [PubMed: 21428688]
13. Stephanopoulos N, Ortony JH, Stupp SI. Self-Assembly for the Synthesis of Functional Biomaterials. Acta Mater. 2013; 61(3):912–930. [PubMed: 23457423]
14. Petersen S, Alonso JM, Specht A, Duodu P, Goeldner M, del Campo A. Phototriggering of cell adhesion by caged cyclic RGD peptides. Angew Chem Int Ed Engl. 2008; 47(17):3192–3195. [PubMed: 18348119]
15. Yeo WS, Yousaf MN, Mrksich M. Dynamic interfaces between cells and surfaces: electroactive substrates that sequentially release and attach cells. J Am Chem Soc. 2003; 125(49):14994–14995. [PubMed: 14653727]
16. Ohmuro-Matsuyama Y, Tatsu Y. Photocontrolled cell adhesion on a surface functionalized with a caged arginine-glycine-aspartate peptide. Angew Chem Int Ed. 2008; 47(39):7527–7529.
17. Liu DB, Xie YY, Shao HW, Jiang XY. Using Azobenzene-Embedded Self-Assembled Monolayers To Photochemically Control Cell Adhesion Reversibly. Angew Chem Int Ed. 2009; 48(24):4406–4408.
18. Wirkner M, Alonso JM, Maus V, Salierno M, Lee TT, Garcia AJ, et al. Triggered cell release from materials using bioadhesive photocleavable linkers. Adv Mater. 2011; 23(34):3907–3910. [PubMed: 21618293]
19. Boekhoven J, Rubert Perez CM, Sur S, Worthy A, Stupp SI. Dynamic Display of Bioactivity through Host-Guest Chemistry. Angew Chem Int Ed Engl. 2013
20. Kloxin AM, Kasko AM, Salinas CN, Anseth KS. Photodegradable hydrogels for dynamic tuning of physical and chemical properties. Science. 2009; 324(5923):59–63. [PubMed: 19342581]
21. Mosiewicz KA, Kolb L, van der Vlies AJ, Martino MM, Lienemann PS, Hubbell JA, et al. In situ cell manipulation through enzymatic hydrogel photopatterning. Nat Mater. 2013; 12(11):1072–1078. [PubMed: 24121990]
22. Elisseeff J, Anseth K, Sims D, McIntosh W, Randolph M, Langer R. Transdermal photopolymerization for minimally invasive implantation. Proc Natl Acad Sci U S A. 1999; 96(6): 3104–3107. [PubMed: 10077644]
23. Anderson JM, Rodriguez A, Chang DT. Foreign body reaction to biomaterials. Semin Immunol. 2008; 20(2):86–100. [PubMed: 18162407]
24. Phelps EA, Enemchukwu NO, Fiore VF, Sy JC, Murthy N, Sulchek TA, et al. Maleimide cross-linked bioactive PEG hydrogel exhibits improved reaction kinetics and cross-linking for cell encapsulation and in situ delivery. Adv Mater. 2012; 24(1):64–70. 62. [PubMed: 22174081]
25. Franz S, Rammelt S, Scharnweber D, Simon JC. Immune responses to implants - a review of the implications for the design of immunomodulatory biomaterials. Biomaterials. 2011; 32(28):6692–6709. [PubMed: 21715002]
26. Phelps EA, Landazuri N, Thule PM, Taylor WR, Garcia AJ. Bioartificial matrices for therapeutic vascularization. Proc Natl Acad Sci U S A. 2010; 107(8):3323–3328. [PubMed: 20080569]
27. Phelps EA, Headen DM, Taylor WR, Thule PM, Garcia AJ. Vasculogenic bio-synthetic hydrogel for enhancement of pancreatic islet engraftment and function in type 1 diabetes. Biomaterials. 2013; 34(19):4602–4611. [PubMed: 23541111]
28. Lynn AD, Blakney AK, Kyriakides TR, Bryant SJ. Temporal progression of the host response to implanted poly(ethylene glycol)-based hydrogels. J Biomed Mater Res A. 2011; 96(4):621–631. [PubMed: 21268236]
29. Dreaden EC, Alkilany AM, Huang X, Murphy CJ, El-Sayed MA. The golden age: gold nanoparticles for biomedicine. Chem Soc Rev. 2012; 41(7):2740–2779. [PubMed: 22109657]
30. Timko BP, Arruebo M, Shankarappa SA, McAlvin JB, Okonkwo OS, Mizrahi B, et al. Near-infrared-actuated devices for remotely controlled drug delivery. Proc Natl Acad Sci U S A. 2014; 111(4):1349–1354. [PubMed: 24474759]

31. Xia Y, Li W, Cobley CM, Chen J, Xia X, Zhang Q, et al. Gold nanocages: from synthesis to theranostic applications. Acc Chem Res. 2011; 44(10):914–924. [PubMed: 21528889]

32. Zaveri TD, Lewis JS, Dolgova NV, Clare-Salzler MJ, Keselowsky BG. Integrin-directed modulation of macrophage responses to biomaterials. Biomaterials. 2014; 35(11):3504–3515. [PubMed: 24462356]

33. Brooks PC, Clark RA, Cheresh DA. Requirement of vascular integrin alpha v beta 3 for angiogenesis. Science. 1994; 264(5158):569–571. [PubMed: 7512751]

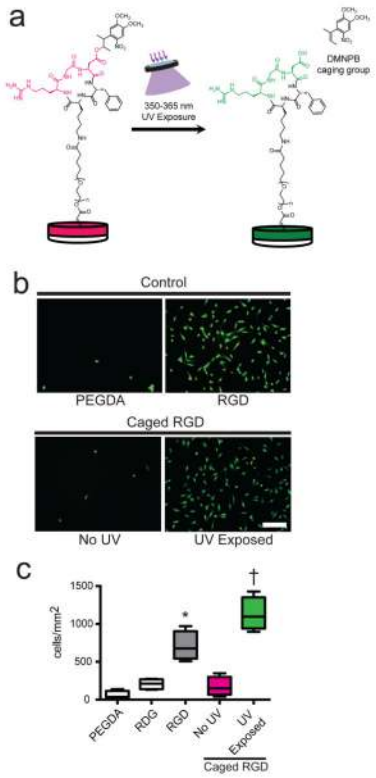

Figure 1. Light-triggered activation of cell adhesion activity of caged RGD peptide on hydrogels

a, Schematic representation of caged RGD peptide-functionalized PEGDA hydrogels. Light exposure at 350–365 nm cleaves UV-labile caging group to present active cyclic RGD peptide. Magenta/green denotes caged/active RGD peptide. **b,** Photographs of fluorescently labeled cells cultured on unmodified PEGDA and peptide-modified hydrogels that were either exposed to UV light or not exposed (scale bar, 300 μm). Hydrogels presenting control RGD peptide and UV-exposed caged RGD peptide supported high levels of adherent cells. Unmodified PEGDA gels and hydrogels presenting RDG scrambled peptide and non-exposed caged RGD peptide supported very low numbers of adherent cells with rounded morphology. **c,** Adherent cell density on hydrogels, box-whisker plot (minimum, 25th percentile, median, 75th percentile, and maximum) for 4 samples per group. Kruskal-Wallis $p < 0.0026$. UV-exposed gels presenting caged RGD supported 4-fold higher adherent cell densities than hydrogels functionalized with caged RGD peptide that were not exposed to UV († $p < 0.01$), surfaces presenting scrambled RDG peptide, and bare PEGDA hydrogels ($p < 0.01$). Cell density was higher on control RGD compared to RDG peptide ($p < 0.05$). No differences in cell adhesion density were observed between UV-exposed caged RGD peptide-presenting gels and hydrogels presenting control RGD peptide ($p = 0.08$).

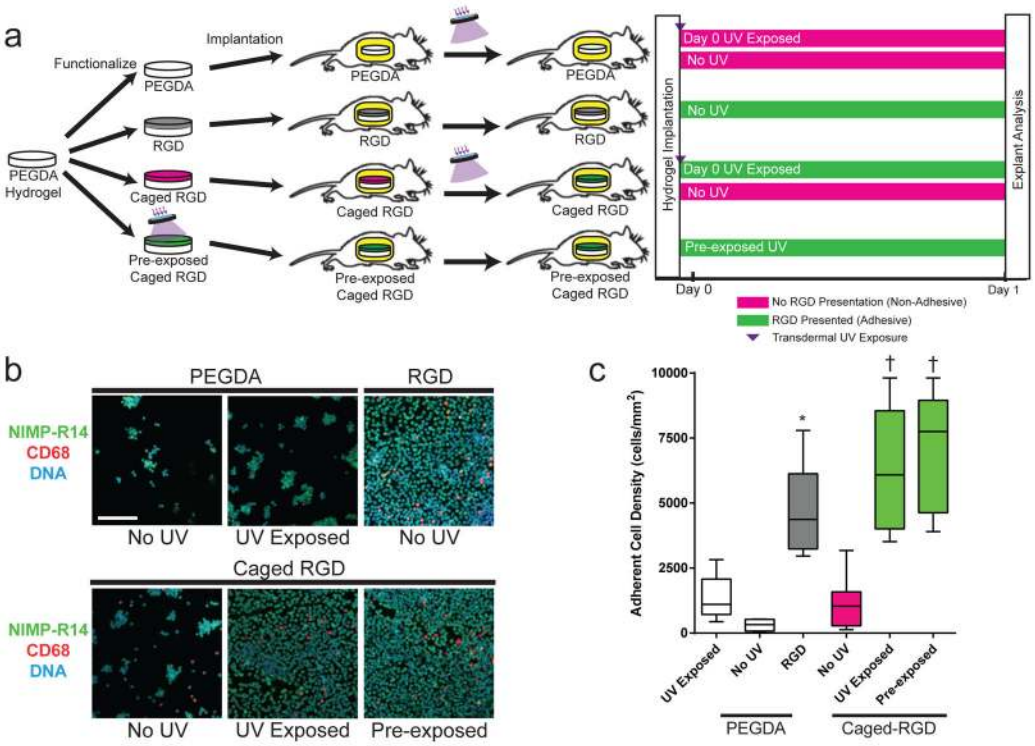

Figure 2. Transdermal activation of *in vivo* inflammatory cell adhesion

a, Schematic representation of timeline for *in vivo* activation of cell adhesion using transdermal UV exposure. **b**, Photographs of explanted hydrogels stained for adherent inflammatory cells (green = NIMP-R14 [neutrophil], magenta = CD68 [macrophage], blue = DAPI [DNA], scale bar, 80 μm). Unfunctionalized PEGDA hydrogels exhibited minimal cell adhesion regardless of UV exposure, whereas hydrogels presenting control RGD peptide supported uniformly high numbers of adherent cells. Hydrogels presenting caged RGD peptide that were not UV-exposed displayed background levels of cell adhesion. In contrast, caged RGD-functionalized gels that were exposed to UV transdermal exhibited high numbers of adherent cells that were uniformly distributed over the biomaterial surface. **c**, Adherent cell density, box-whisker plot (minimum, 25th percentile, median, 75th percentile, and maximum) for 6–8 mice per group, demonstrating light-based triggering of inflammatory cell adhesion to caged RGD-presenting implants. ANOVA $p < 0.0001$, * $p < 0.05$ vs. UV-exposed PEGDA, † $p < 0.001$ vs. No UV Caged RGD.

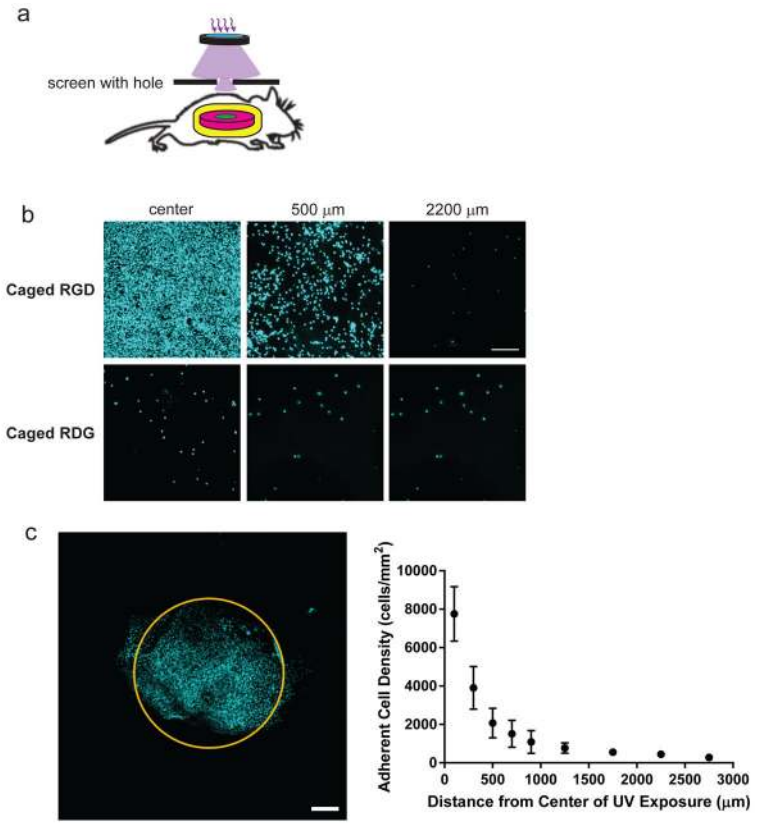

Figure 3. Light-triggered spatial patterning of *in vivo* cell adhesion

a, Schematic representation of patterning experiment using transdermal UV exposure through a mask. **b**, Photographs of explanted hydrogels stained for adherent cell nuclei for caged RGD and RDG presenting hydrogels at different distances from the center of irradiation (DAPI, color coded cyan, scale bar, 40 μm). **c**, Left: Composite image of photographs of adherent cell nuclei (cyan). Yellow circle designates exposure spot (scale bar, 200 μm). Right: Adherent cell density vs. distance away from irradiation point. Data represent mean ± standard error for hydrogels explanted for 5 mice per group.

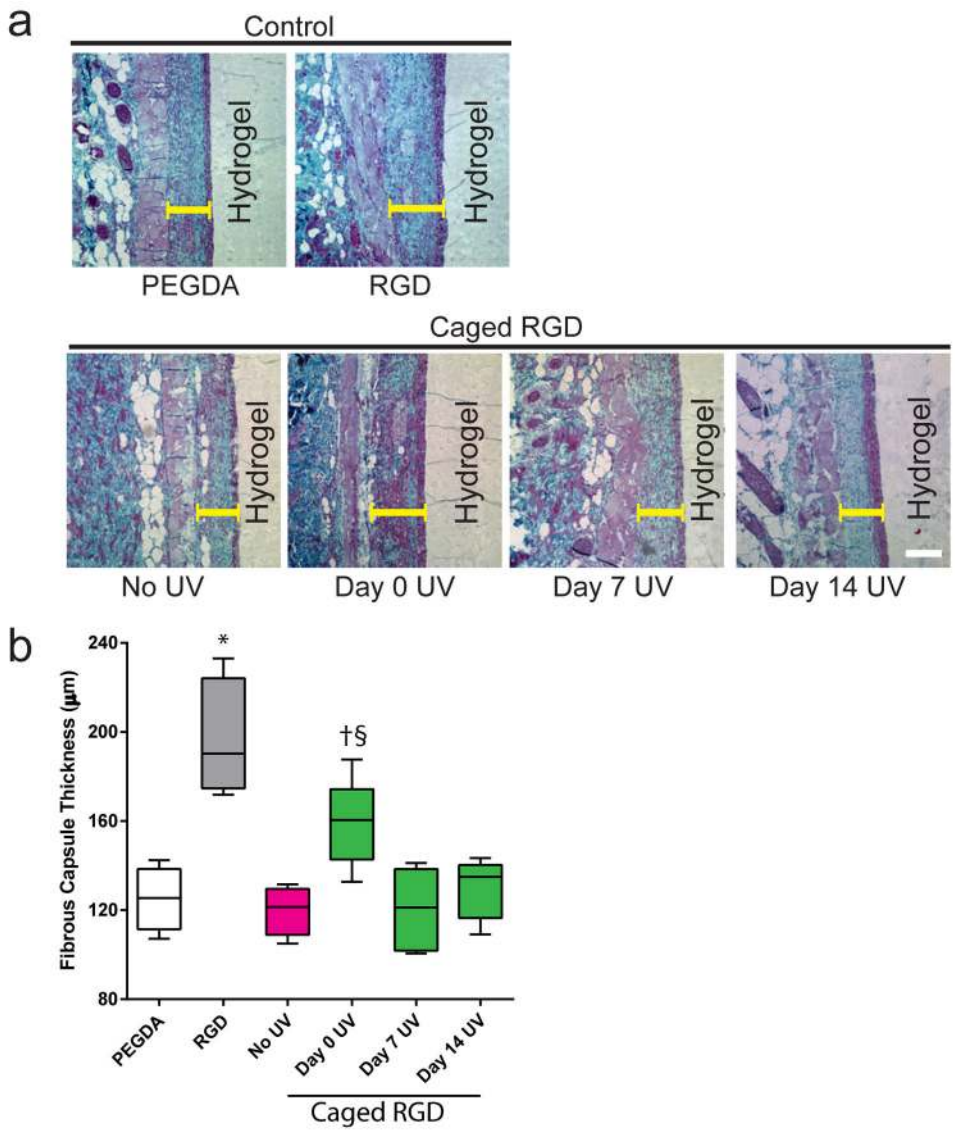

Figure 4. Time-regulated *in vivo* activation of RGD peptide modulates fibrous encapsulation of implanted biomaterials

Unfunctionalized PEGDA hydrogels and gels presenting either control RGD or caged RGD peptides were implanted subcutaneously and at prescribed time points were exposed to UV transdermally. Biomaterials and associated tissue were explanted at 28 days. **a**, Photographs of plastic-embedded sections stained by Mason's trichrome of fibrous capsule formation around implanted hydrogels at 28 days (scale bar, 100 μm). Yellow bars denote fibrous capsule. **b**, Fibrous capsule thickness around implanted hydrogels, box-whisker plot (minimum, 25th percentile, median, 75th percentile, and maximum) for 4–6 mice per group. ANOVA $p < 0.0001$, * $p < 0.001$ vs. PEGDA, † $p < 0.01$ vs. No UV Caged RGD, § $p < 0.05$ vs. Day 0 Caged RGD.

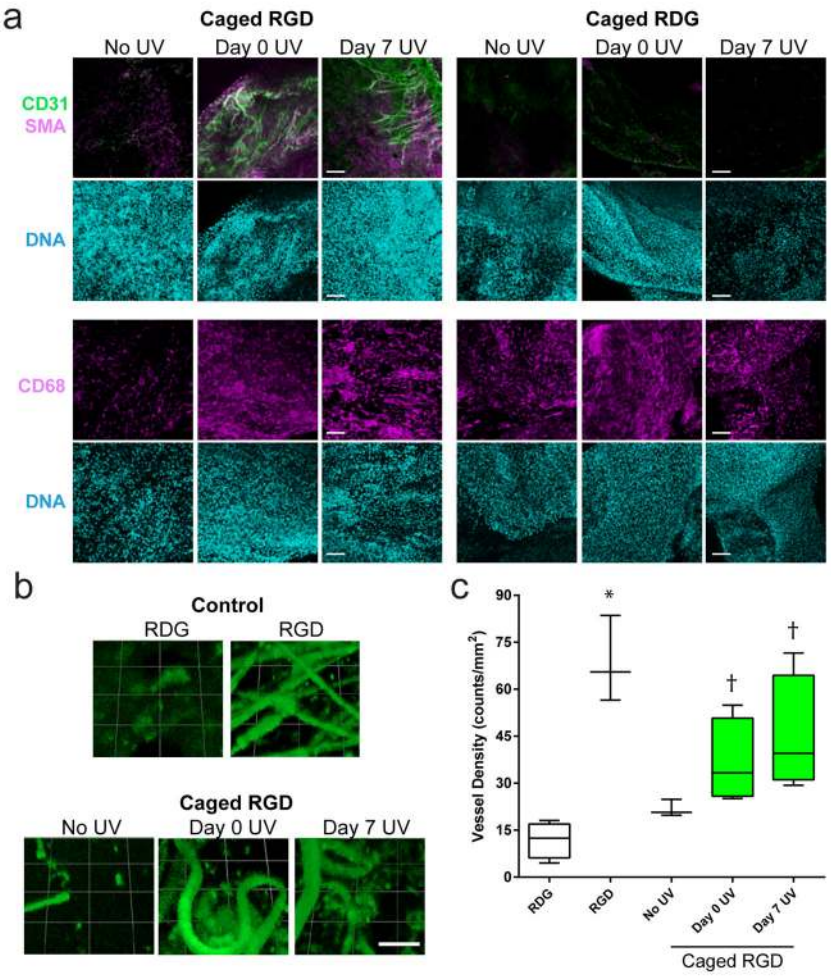

Figure 5. Light-based activation of cell adhesive peptide promotes vascularization of implanted biomaterials

a, Immunostaining images for hydrogels presenting caged RGD or caged RDG peptide for different UV exposure conditions. Top: green = CD31 [endothelial cell], magenta = αSMA [smooth muscle cell], blue = DAPI [DNA], scale bar, 100 μm. Bottom: magenta = CD68 [macrophage], blue = DAPI [DNA], scale bar, 100 μm. **b**, Fluorescent images of blood vessel ingrowth (green) into PEG-maleimide hydrogels implanted subcutaneously at 14 days (scale bar, 100 μm). PEG-maleimide hydrogels presenting peptides were implanted subcutaneously and exposed to UV transdermally at selected time points. Mice were perfused with DyLight488-conjugated tomato lectin at sacrifice to label functional blood vessels. Hydrogels presenting caged RGD peptides which were exposed to UV transdermally at Day 0 and Day 7 exhibited robust blood vessel growth, similar to gels presenting control RGD. Hydrogels functionalized with scrambled RDG peptide or caged RGD peptide that was not exposed to UV displayed minimal blood vessel infiltration. **c**, Blood vessel density, box-whisker plot (minimum, 25th percentile, median, 75th percentile, and maximum) for 4 mice per group for caged RGD conditions, 3 mice per group for control peptides. Kruskal-Wallis $p < 0.01$, * $p < 0.01$ vs. RDG, † $p < 0.05$ vs. No UV Caged RGD.